



Published in final edited form as:

ChemMedChem. 2017 December 19; 12(24): 2022–2029. doi:10.1002/cmdc.201700630.

Synthesis and biological evaluation of stilbene analogs as Hsp90 C-terminal inhibitors

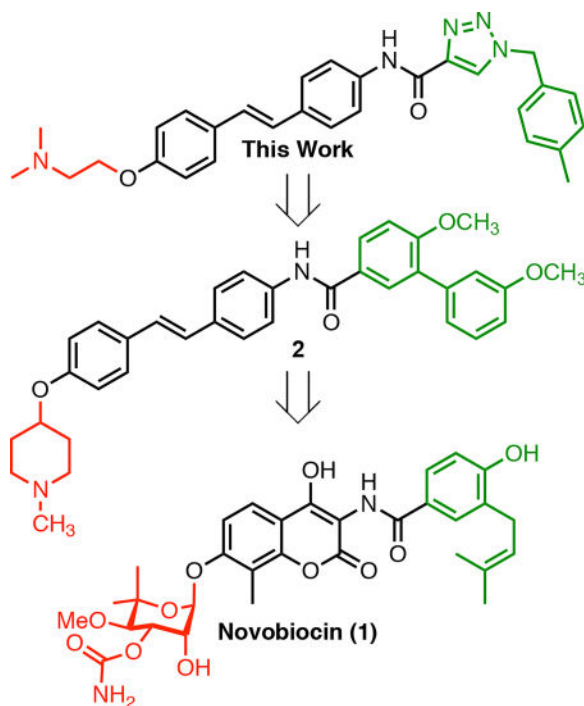
Katherine M. Byrd, Caitlin N. Kent, and Brian S. J. Blagg*

Department of Chemistry and Biochemistry, University of Notre Dame, 251 Nieuwland Science Hall, Notre Dame, IN 46556, USA

Abstract

The design, synthesis and biological evaluation of stilbene-based novobiocin analogs is reported. Replacement of the biaryl amide side chain with a triazole side chain produced compounds that exhibited good anti-proliferative activities. Hsp90 inhibition was observed when N-methyl piperidine was replaced with acyclic tertiary amines on the stilbene analogs that also contain a triazole-derived side chain. These studies revealed that ~24 Å is the optimal length for compounds that exhibit good anti-proliferative activity as a result of Hsp90 inhibition.

Table of Contents



This work focused on the design and biological evaluation of stilbene-based novobiocin analogs. Initial efforts revealed the stilbene moiety as the optimal core. These studies revealed that

replacement of the biaryl amide side chain with triazole containing analogs and tertiary amines on the stilbene core produced more efficacious compounds as confirmed by EC₅₀ values and western blot analyses.

Keywords

Heat Shock Protein 90; Stilbene; C-terminal inhibitors; Anti-cancer agents

Introduction

Heat shock protein 90 kDa (Hsp90) is a molecular chaperone that folds polypeptides and denatured proteins into their bioactive conformation.^[1] In humans, Hsp90 exists as four isoforms: Hsp90 α , Hsp90 β , glucose-regulated protein 94 kDa (Grp94), and tumor necrosis receptor-associated protein 1 (Trap1). Hsp90 α and Hsp90 β are localized to the cytoplasm, whereas Grp94 resides in the endoplasmic reticulum, and Trap1 is localized within the mitochondria.^[2,3] Structurally, these isoforms are homodimers, whose monomeric unit consists of an N-terminal ATP-binding motif, a middle domain, and a C-terminal dimerization motif.^[4,5] Hsp90 is responsible for the activation/maturation of more than 300 client proteins, many of which are associated with the 10 hallmarks of cancer.^[6–8] Since Hsp90 inhibition results in the simultaneous degradation of multiple oncogenic targets, it has emerged as a novel target for to development of anti-cancer agents. Additionally, studies have shown that Hsp90 is overexpressed in cancer, which provides an additional opportunity to selectively target Hsp90 in cancer cells versus normal tissue.^[9–11]

Initial efforts to develop Hsp90 inhibitors for the treatment of cancer focused on compounds that bind the Hsp90 N-terminus. These efforts led to the identification of twenty Hsp90 N-terminal inhibitors that have now been investigated in a clinical setting.^[12–15] To date, no Hsp90 inhibitor has been approved by the FDA for the treatment of cancer. Unfortunately, these studies were plagued by dosing difficulties and some toxicity issues associated with induction of the pro-survival heat shock response at the same concentration that inhibits client protein folding.^[16] In order to address these issues, Hsp90 isoformselective inhibitors have been sought to limit and identify potential on-target toxicities.^[17] Recently, it was demonstrated that selective inhibition of Hsp90 β can inhibit a number of cancers without concomitant induction of Hsp90.^[18]

Hsp90 C-terminal inhibitors have been shown to induce Hsp90 client protein degradation without concomitant induction of the heat shock response.^[19] Therefore, this approach represents an attractive alternative to Hsp90 N-terminal inhibition. Although there is no co-crystal structure of the Hsp90 C-terminus bound to inhibitors,^[20] drug discovery efforts have led to the identification of Hsp90 C-terminal inhibitors that exhibit excellent anti-proliferative activity against a variety of cancers.^[21] Those Hsp90 C-terminal inhibitors have been developed by elucidation and evaluation of structure-activity relationship (SAR) studies on novobiocin (1), which was the first Hsp90 C-terminal inhibitor identified.^[22–24] Previous studies also determined the optimal distance and angle between the N-methyl piperidine and biaryl amide side chain^[25] which revealed that the most efficacious anti-

proliferative and Hsp90 inhibitory activities were obtained when the distance was between 7.7 to 11.8 Å and the angle was ~180° (Figure 1). In fact, stilbene **2** was identified as the most efficacious inhibitor that exhibited both potent anti-proliferative and Hsp90 inhibitory activity. Therefore, the focus of this work was to optimize **2**, identify structure-activity relationships, and obtain more efficacious compounds.

Results and Discussion

Synthesis and biological evaluation of stilbene core analogs

Initial efforts to modify **2** consisted of three approaches (Figure 2): The first approach was to restrict rotation of the phenyl rings within the stilbene core, thus prohibiting the entropic penalty observed upon binding. Such compounds could provide insight into preferred orientation of the phenyl ring upon binding Hsp90. The first ring-constrained analogs were comprised of a 6-phenyl-7,8-dihydronaphthalene core, which allowed rotation of one phenyl ring. The second approach sought to investigate the electronic effects by enlisting a Topliss tree approach^[26] to dictate subsequent modification. The final approach was to modify orientation of the N-methyl piperidine and biaryl amide side chain through the incorporation of a cyclopropane ring or inclusion of a saturated phenyl ring.

Synthesis of ring-constrained analogs

Synthesis of **3** commenced via a Suzuki coupling between vinyl triflate **8**^[27] and 4-hydroxyphenylboronic acid to produce **9** in 45% yield (Scheme 1). N-methyl-4-piperidinol (**10**) was then coupled with **9** via a Mitsunobu etherification.^[28] Following removal of the Boc-protecting group, the resulting aniline was coupled with acid chloride **12** to yield **3** in 39% over both steps. Compound **3** was subsequently subjected to hydrogenation conditions to yield the saturated derivative, **13**.

Preparation of **4** was initiated by installation of a methoxymethyl (MOM) protecting group onto 6-hydroxy-2-tetralone (Scheme 2). Tetralone **14** was first converted to the vinyl triflate and then immediately coupled with 4-nitrophenylboronic acid, to form **16**. Upon removal of the protecting group present in **16**, the resulting phenol was coupled with N-methyl-4-piperidinol through a Mitsunobu etherification reaction. Following reduction of the nitro group in **17** to the corresponding aniline, the aniline was treated with acid chloride **12** to form **4** in 50% yield. Hydrogenation of **4** led to saturated derivative **18**, in 58% yield.

Synthesis of analogs to study electronic effects

The first stilbene derivatives synthesized contained a chloride group in the ortho- or meta-position of the amide substituted phenyl ring (See supporting information for synthesis). Since the chloro-containing derivatives were less active than the parent compound, methoxy-substituted stilbenes were synthesized according to the Topliss approach (Scheme 3). Stilbenes **20a/b** were synthesized via a Heck coupling between styrene **19**^[29] and the corresponding nitrobenzenes. Upon reduction of the nitro groups in **20a/b**, the resulting anilines were coupled with carboxylic acid **21** to form amides **22a/b**. Following removal of the MOM group, the corresponding phenols were coupled with N-methyl-4-piperidinol.

Synthesis of saturated analogs of **2**

Synthesis of the cyclopropane analog^[30] began via cyclopropanation of stilbene **24**.^[31,32] (Scheme 4) Following demethylation of **25**, a methoxymethyl group was placed onto the resulting phenol. Aryl bromide **26** was coupled^[33] with amide **27** via Hartwig-Buchwald amidation to form **28**. After removal of the methoxymethyl ether, the corresponding phenol was coupled with N-methyl-4-piperidinol to form the final product, **6**.

Preparation of the saturated analog of **2** commenced via a Horner-Wadsworth-Emmons reaction between phosphonate **29** and aldehyde **30**,^[34] to form **31** (Scheme 5). After removal of the ketal on **31**, the resulting ketone **32** was subjected to a deprotection-protection protocol to produce **33**. Syn alcohol **34** was obtained via the treatment of **33** with L-Selectride. Following activation of the alcohol with methanesulfonyl chloride, the resulting mesylate was displaced to form azide **35**. Amide **36** was then formed by reduction of azide **35** to form the corresponding amine, which was subsequently coupled with carboxylic acid **21** to give **36**. Removal of the toluenesulfonate ester and coupling of the resulting phenol with N-methyl-4-piperidinol completed the preparation of **7**.

These initial analogs were evaluated against three cancer cell lines: MCF-7 (estrogen receptor positive breast cancer cells), SKBr3 (estrogen receptor negative, HER2 overexpressing breast cancer cells) and HCT-116 (human colon cancer cells). (Table 1) Restriction of rotation of either phenyl ring resulted in a significant or complete loss of anti-proliferative activity across all three cancer cell lines. These results suggest that the addition of two carbons at the center of the stilbene core may cause a steric clash with Hsp90. The addition of a chloro or methoxy group also caused a significant loss in anti-proliferative activity, as compared to the parent compound. The saturated analogs manifested the most efficacious anti-proliferative activities, and the activity of **7** was comparable to parent compound **2**. In order to determine whether the anti-proliferative activities manifested by the saturated analogs were the result of Hsp90 inhibition, western blot analyses were performed on MCF-7 cell lysates treated with **6** and **7** for 24 hours (Figure 1S). Neither compound was able to induce Hsp90 dependent client protein degradation at concentrations that mirror the IC₅₀ values. Overall, the results from these compounds show that stilbene **2** remains the optimal core for the design of future analogs.

Second-generation stilbene analogs

It was important to change either the N-methyl piperidine or biaryl amide side chain based on the information gained from the first generation of compounds. Since the N-methyl piperidine and biaryl amide side chain were optimized for the coumarin and biphenyl scaffold, appendages on both sides of the stilbene core were investigated.

Investigation of replacements for the N-methyl piperidine and biaryl amide side chain

Previous optimization studies on the noviose sugar and prenylated amide side chain of novobiocin (**1**) provided insight towards the inclusion of N-methyl piperidine and the biaryl amide side chain. For example, such studies revealed that the best anti-proliferative activities were obtained when the noviose sugar was replaced with a tertiary amine.^[22b] Subsequent studies have shown that the tertiary amine (cyclic versus acyclic) can play a significant role

in binding the Hsp90 C-terminal domain.^[35] Therefore, various acyclic tertiary amines were investigated with this stilbene core. In terms of the biaryl amide side chain, work has been done to probe the utility of each aromatic ring on the amide side chain and alternative aromatic systems have been identified that can replace the biaryl amide side chain. Of the systems investigated from the literature, a triazole-containing amide side chain was shown to manifest the most efficacious activity against multiple cancer cell lines.^[22c] Therefore, triazole-based amide side chains were investigated as replacements for the biaryl amide side chain in this study.

Scheme 6 illustrates the general synthetic route used to construct the triazole-based stilbene analogs. 4-Nitro-4'-hydroxystilbene was protected with a methoxymethyl group to yield **39**. Next, the nitro group was reduced to the corresponding aniline, which was then coupled with the requisite carboxylic acid to form the resulting amide. The protecting group on the amide was removed before the appropriate tertiary amine was then coupled with the phenol via a Mitsunobu etherification or S_N2 reaction.

Replacement of the biaryl amide side chain with the triazole moiety caused a significant increase in anti-proliferative activity against all of the investigated cell lines (Table 2). Regardless of **R**, compounds containing the triazole and 4-methylbenzyl group (**C**) were more potent than the benzyl (**B**) substituted derivatives. When N-methyl-piperidine (**X**) was replaced with 3-(dimethylamino)propane (**Y**), the activity decreased as in **47**, while the activity of **46** was similar to **44**. Interestingly, when the shorter 2-(dimethylamino)ethane (**Z**) was added onto the stilbene core, an improvement in anti-proliferative activity was observed for both triazole-containing compounds (**48** and **49**). This data suggests that a limited amount of space exists within the binding pocket. Once a compound exceeds that defined space, then the anti-proliferative activities decrease. For example, the activities manifested by **49** are better than the activities exhibited by **47**, suggesting that **47** is too large to fit within the Hsp90 C-terminal binding pocket. In order to independently probe the effect of the acyclic amine on anti-proliferative activity, **50** was tested against all of the cancer cell lines. Since **50** is significantly less active than **2**, it is clear that the increase in anti-proliferative activity is due to replacement of the biaryl amide side chain with the triazole moiety.

Western blot analyses of MCF-7 cell lysates incubated with **44** and **45** for 24 hours were conducted to determine whether the observed anti-proliferative activities resulted from Hsp90 inhibition (Figure 3). For **44**, a dose-dependent degradation of Hsp90-dependent client proteins was observed, whereas no degradation of Hsp90 client proteins was observed for **45**. The western blot analysis of **46** and **47** showed that **46**, but not **47**, induced client protein degradation (Figure 4). On the other hand, western blot analysis of **48** and **49** revealed that **49** was able to induce Hsp90 client protein degradation. This data supports that there is an overall optimal length for occupancy of the Hsp90 C-terminal binding pocket. As shown in Figure 5, the best compounds (**46** and **49**) are ~ 24 Å in length. If the compound is too long (**47**) or too short (**48**), then the compound is unable to inhibit Hsp90 and induce client protein degradation. The improvement in Hsp90 inhibition by **46** and **49** reveals that the incorporation of a flexible 3-(dimethylamino)alkyl group can produce better interactions with Hsp90 for this particular scaffold.

Conclusions

In an effort to optimize **2**, structure-activity relationships were elucidated for 17 analogs, which revealed the stilbene core to be optimal for these compounds. Replacement of the biaryl amide side chain with a triazole-containing group improved anti-proliferative activity. In addition, replacement of the N-methyl piperidine with a (dimethylamino)alkyl group led to Hsp90 inhibition. The overall length of the best Hsp90 inhibitors was 24 Å.

Experimental Section

¹H NMR were recorded at 400 or 500 MHz (Bruker DRX- 400 Bruker with a H/C/P/F QNP gradient probe) spectrometer and ¹³C NMR spectra were recorded at 125 MHz (Bruker DRX 500 with broadband, inverse triple resonance, and high resolution magic angle spinning HR-MA probe spectrometer); chemical shifts are reported in δ (ppm) relative to the internal reference CDCl₃ (CDCl₃, 7.26 ppm). FAB (HRMS) spectra were recorded with a LCT Premier (Waters Corp., Milford, MA) spectrometer and IR spectra were recorded on a Magna FT-IR spectrometer (Nicolet Instrument Corporation, Madison, WI). The purity of all compounds was determined to be >95% as determined by ¹H NMR and ¹³C NMR spectra, unless otherwise noted. TLC was performed on glass- backed silica gel plates (Uniplate) with spots visualized by UV light. All solvents were reagent grade and, when necessary, were purified and dried by standard methods. Concentration of solutions after reactions and extractions involved the use of a rotary evaporator operating at reduced pressure. Detailed experimental procedures can be found in the supporting information.

Supplementary Material

Refer to Web version on PubMed Central for supplementary material.

Acknowledgments

The authors gratefully acknowledge support of this project by the National Cancer Institute of the National Institutes of Health, CA120458 and CA167079 (KMB) and NIH Dynamic Aspects of Chemical Biology, T32 GM08545 (CNK).

References

1. Trepel J, Mollapour M, Giaccone G, Neckers L. *Nature Rev. Cancer*. 2010; 10:537–549. [PubMed: 20651736]
2. Sreedhar AS, Kalmar E, Csermely P, Shen Y. *FEBS Lett*. 2004; 562:11–15. [PubMed: 15069952]
3. Seo YH. *Arch. Pharm. Res*. 2015; 38:1582–1590. [PubMed: 26195286]
4. Schopf FH, Biebl MM, Buchner J. *Nature Rev. Mol. Cell Biol*. 2017; 18:345–360. [PubMed: 28429788]
5. Pearl LH. *Biopolymers*. 2016; 105:594–607. [PubMed: 26991466]
6. Hanahan D, Weinberg RA. *Cell*. 2011; 144:646–674. [PubMed: 21376230]
7. Hanahan D, Weinberg RA. *Cell*. 2000; 100:57–70. [PubMed: 10647931]
8. Miyata Y, Nakamoto H, Neckers L. *Current Pharmaceutical Design*. 2013; 19:347–365. [PubMed: 22920906]
9. a) Picard D. *Cell. Mol. Life Sci*. 2002; 59:1640–1648. [PubMed: 12475174] b) Issacs JS, Xu W, Neckers L. *Cancer Cell*. 2003; 3:213–217. [PubMed: 12676580] c) Pratt WB, Toft DO. *Exp. Biol*.

- Med. 2003; 228:111–133.d) Whitesell L, Lindquist SL. *Nature Rev. Cancer*. 2005; 5:761–772. [PubMed: 16175177]
10. Moser C, Lang SA, Stoeltzing O. *Anticancer Res*. 2009; 29:2031–42. [PubMed: 19528462]
11. Koga F, Kihara K, Nechers L. *Anticancer Res*. 2009; 29:797–807. [PubMed: 19414312]
12. Franke J, Eichner S, Zeilinger C, Kirschning A. *Nat. Prod. Rep*. 2013; 30:1299–1323. [PubMed: 23934201]
13. Khandelwal A, Crowley V, Blagg BSJ. *Med. Res. Rev*. 2015; 35:92–118.
14. Wang M, Shen A, Zhang C, Song Z, Ai J, Liu H, Sun L, Ding J, Geng M, Zhang A. *J. Med. Chem*. 2016; 59:5563–5586. [PubMed: 26844689]
15. Jhaveri K, Modi S. *Onco Targets Ther*. 2015; 8:1849–1858. [PubMed: 26244021]
16. Hong Banerji U, Tavana B, George GC, Aaron J, Kurzock R. *Cancer Treatment Reviews*. 2013; 39:375–387. [PubMed: 23199899]
17. a) Ernst JT, Neubert T, Liu M, Sperry S, Zuccola H, Turnbull A, Fleck B, Kargo W, Woody L, Chiang P, Tran D, Chen W, Snyder P, Alcacio T, Nezami A, Reynolds J, Alvi K, Goulet L, Stamos D. *J. Med. Chem*. 2014; 57:3382–3400. [PubMed: 24673104] b) Mishra SJ, Ghosh S, Stothert AR, Dickey CA, Blagg BSJ. *ACS Chem. Biol*. 2017; 12:244–253. [PubMed: 27959508] c) Duerfeldt AS, Peterson LB, Maynard JC, Ng CL, Eletto D, Ostrovsky O. *J. Am. Chem. Soc*. 2012; 134:9796–9804. [PubMed: 22642269] d) Patel PD, Yan P, Seidler PM, Patel HJ, Sun W, Yang C, Que NS, Taldone T, Finotti P, Stephani RA, Gewirth DT, Chiosis G. *Nat. Chem. Biol*. 2013; 9:677–684. [PubMed: 23995768] e) Crowley VM, Khandelwal A, Mishra S, Stothert AR, Huard DJE, Zhao J, Muth A, Duerfeldt AS, Kizziah JL, Lieberman RL, Dickey CA, Blagg BSJ. *J. Med. Chem*. 2016; 59:3471–3488. [PubMed: 27003516]
18. Khandelwal A, Kent CN, Balch M, Peng S, Mishra SJ, Deng J, Day VW, Liu W, Holzbeierlein JM, Matts R, Blagg BSJ. *Nat. Commun*. 2017 Accepted.
19. a) Shelton SN, Shawgo ME, Comer SB, Lu Y, Donnelly AC, Szabla K, Tanol M, Vielhauer GA, Rajewski RA, Matts RL, Blagg BS, Robertson JD. *Mol. Pharmacol*. 2009; 76:1314–1322. [PubMed: 19741006] b) Conde R, Belak ZR, Nair M, O’Carroll RF, Ovsenek N. *Biochem. Cell Biol*. 2009; 87:845–851. [PubMed: 19935870]
20. a) Matts RL, Dixit A, Peterson LB, Sun L, Voruganti S, Kalyanaraman P, Hartson SD, Verkhivker GM, Blagg BSJ. *ACS Chem. Biol*. 2011; 6:800–807. [PubMed: 21548602] b) Moroni E, Zhao H, Blagg BSJ, Colombo G. *J. Chem. Inf. Model*. 2014; 54:195–208. [PubMed: 24397468] c) Sattin S, Tao J, Vettoretti G, Moroni E, Pennati M, Lopergolo A, Morelli L, Bugatti A, Zuehlke A, Moses M, Prince T, Kijima T, Beebe K, Rusnati M, Neckers L, Zaffaroni N, Agard DA, Bernardi A, Colombo G. *Chem. Eur. J*. 2015; 21:13598–15608. [PubMed: 26286886]
21. a) Strocchia M, Terracciano S, Chini MG, Vassallo A, Vaccaro MC, Dal Piaz F, Leone A, Riccio R, Bruno I, Bifulco G. *Chem Commun*. 2015; 51:3850–3853. b) Terracciano S, Foglia A, Chini MG, Vaccaro MC, Russo A, Dal Piaz F, Saturnino C, Riccio R, Bifulco G, Bruno I. *RSC Adv*. 2016; 6:82330–82340. c) Wang Y, McAlpine SR. *Org. Biomol. Chem*. 2015; 13:4627–4631. [PubMed: 25711919] d) Wang Y, McAlpine SR. *Chem. Commun*. 2015; 51:1410–1403. e) Gavenonis J, Jonas NE, Kritzer JA. *Bioorg. Med. Chem*. 2014; 22:3989–3993. [PubMed: 24984936]
22. a) Garg G, Zhao H, Blagg BS. *J. ACS Med. Chem. Lett*. 2015; 6:204–209. b) Hall JA, Forsberg LK, Blagg BSJ. *Future Med. Chem*. 2014; 6:1587–1605. [PubMed: 25367392] c) Zhao H, Zhao H, Hall JA, Brown D, Brandes E, Bazzill J, Grogan PT, Subramanian C, Vielhauer G, Cohen MS, Blagg BSJ. *MedChemComm*. 2014; 5:1317–1323. [PubMed: 25328661] d) Zhao H, Moroni E, Colombo G, Blagg BS. *J. ACS Med. Chem. Lett*. 2014; 5:84–88. e) Zhao H, Yan B, Peterson LB, Blagg BS. *J. ACS Med. Chem. Lett*. 2012; 3:327–331. f) Kusuma BR, Peterson LB, Zhao H, Vielhauer G, Holzbeierlein, Blagg BSJ. *J. Med. Chem*. 2011; 54:6234–6253. [PubMed: 21861487] g) Burlison JA, Neckers L, Smith AB, Maxwell A, Blagg BSJ. *J. Am. Chem. Soc*. 2006; 128:15529–15536. [PubMed: 17132020] h) Burlison JA, Blagg BS. *J. Org. Lett*. 2006; 8:4855–4858. i) Yu XM, Shen G, Neckers L, Blake H, Holzbeierlein J, Cronk B, Blagg BSJ. *J. Am. Chem. Soc*. 2005; 127:12778–12779. [PubMed: 16159253] j) Davis RE, Zhang Z, Blagg BSJ. *MedChemComm*. 2017; 8:593–598. [PubMed: 28533894] k) Garg G, Zhao H, Blagg BS. *J. Bioorg. Med. Chem*. 2017; 25:451–457.
23. a) Zhao H, Kusuma BR, Blagg BSJ. *ACS Med. Chem. Lett*. 2010; 1:311–315. [PubMed: 21904660] b) Zhao H, Donnelly AC, Kusuma BR, Brandt GEL, Brown D, Rajewski RA,

- Vielhauer G, Holzbeierlein J, Cohen MS, Blagg BSJ. *J. Med. Chem.* 2011; 54:3839–3853. [PubMed: 21553822]
24. a) Zhao H, Garg G, Zhao J, Moroni E, Girgis A, Franco LS, Singh S, Colombo G, Blagg BSJ. *Eur. J. Med. Chem.* 2015; 89:442–466. [PubMed: 25462258] b) Zhao H, Anyika M, Girgis A, Blagg BSJ. *Bioorg. Med. Chem. Lett.* 2014; 24:3633–3637. [PubMed: 24953820]
25. Byrd KM, Subramanian C, Sanchez J, Motiwala HF, Liu W, Cohen MS, Holzbeierlein J, Blagg BSJ. *Chem. Eur. J.* 2016; 22:6921–6931. [PubMed: 27037933]
26. Topliss JG. *J. Med. Chem.* 1972; 15:1006–1011. [PubMed: 5069767]
27. Boinapally S, Huang B, Abe M, Katan C, Noguchi J, Watanabe S, Kasai H, Xue B, Kobayashi T. *J. Org. Chem.* 2014; 79:7822–7830. [PubMed: 25101898]
28. Tsunoda T, Yamamiya Y, Kawamura Y, Itô S. *Tetrahedron Lett.* 1995; 36:2529–2530.
29. Singh M, Argade N. *Synthesis.* 2012; 44:2895–2902.
30. The authors tried using 4-nitro-4'-hydroxystilbene as the starting material for the cyclopropanation but none of the standard reactions work. Due to safety concerns, diazomethane was not used for the cyclopropanation of this compound.
31. Skhiri A, Salem RB, Soulé J, Doucet H. *Synthesis.* 2016; 48:3097–3106.
32. Pitts CR, Ling B, Synder JA, Bragg AE, Lectka T. *J. Am. Chem. Soc.* 2016; 138:6598–6609. [PubMed: 27136383]
33. Huang X, Anderson KW, Zim D, Jiang L, Klapars A, Buchwald SL. *J. Am. Chem. Soc.* 2003; 125:6653–6655. [PubMed: 12769573]
34. Kitbunnadaj R, Hoffmann M, Fratantoni SA, Bongers G, Bakker RA, Wieland K, Jilali A, De Esch IJP, Menge WMPB, Timmerman H, Leurs R. *Bioorg. Med. Chem.* 2005; 13:6309–6323. [PubMed: 16213736]
35. Garg G, Forsberg LF, Zhao H, Blagg BSJ. *Chem. Eur. J.* 2017; :10.doi: 10.1002/chem.201703206
36. ChemBioUltra Version 13.0 (Cambridgesoft)
37. Maestro Version 11.2014 (Schrodinger)

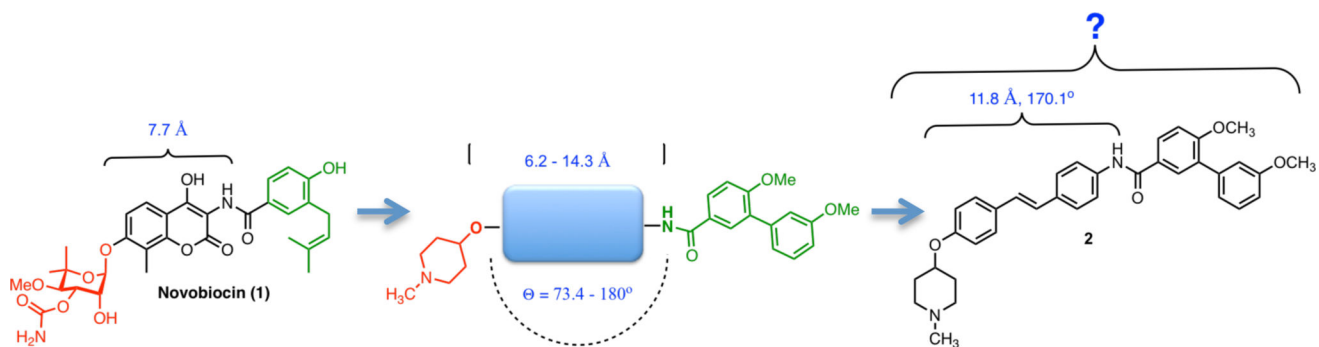


Figure 1.
Previous Hsp90 inhibitors

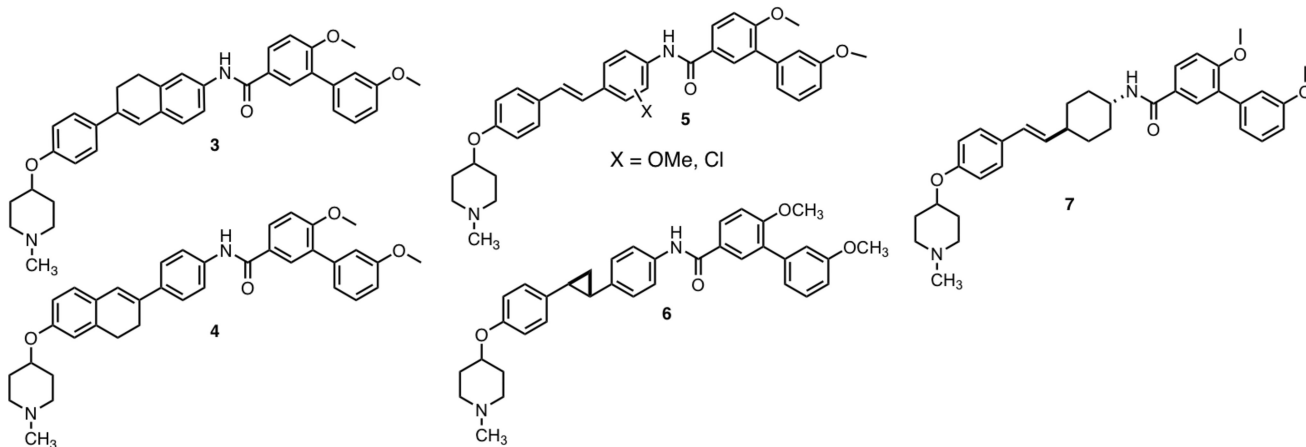
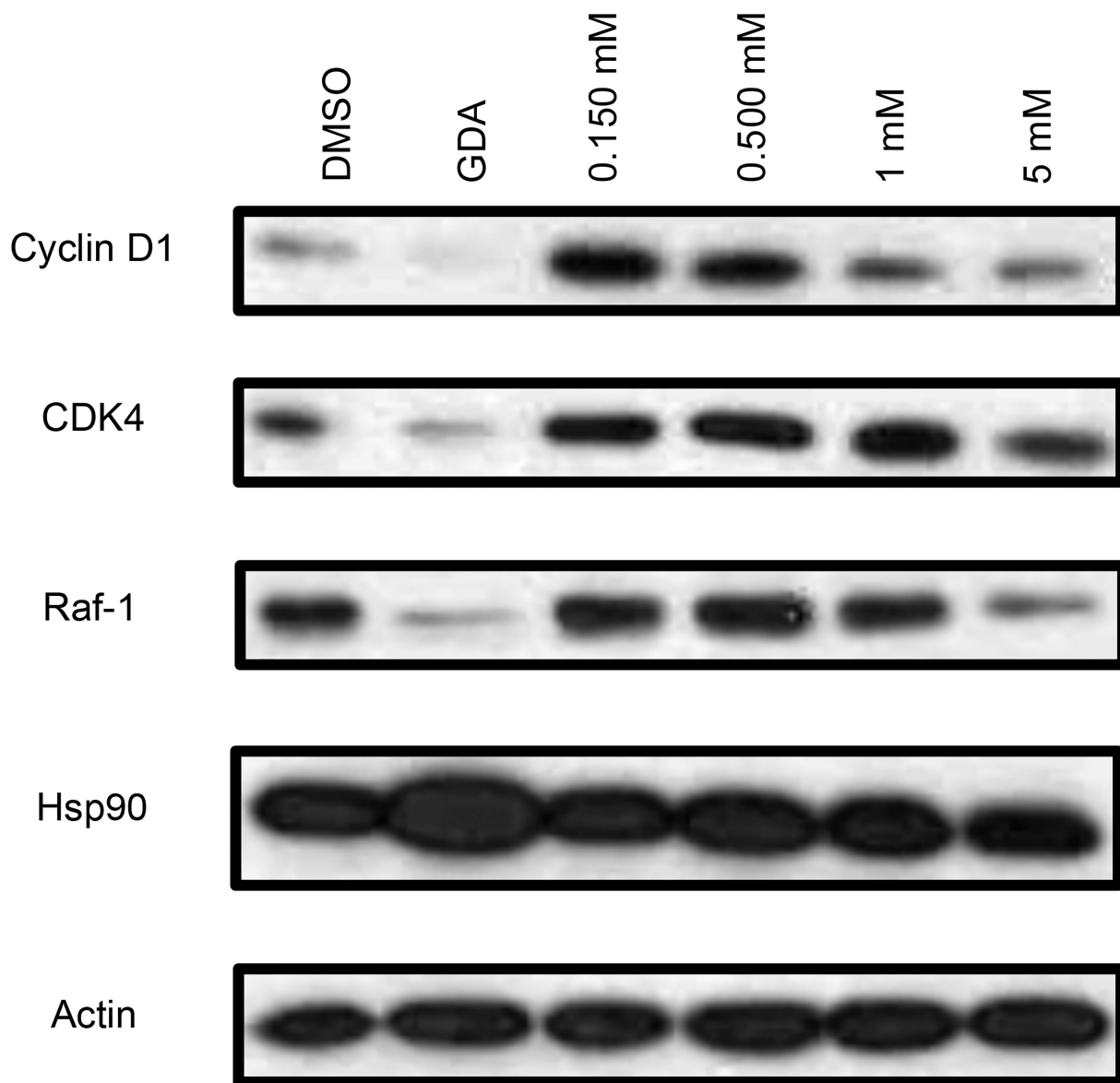


Figure 2.
Initial analogs of **2**

A.



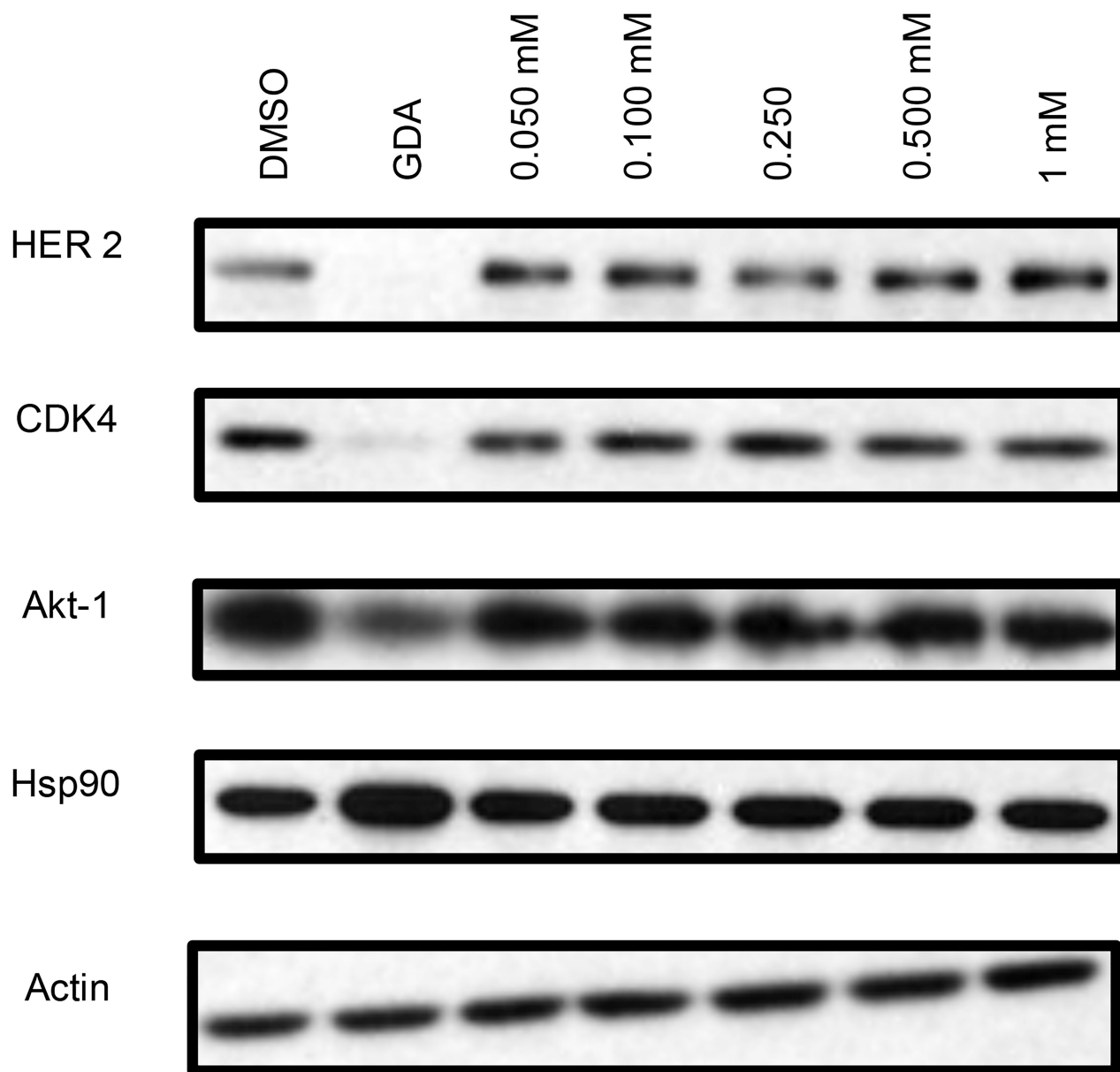
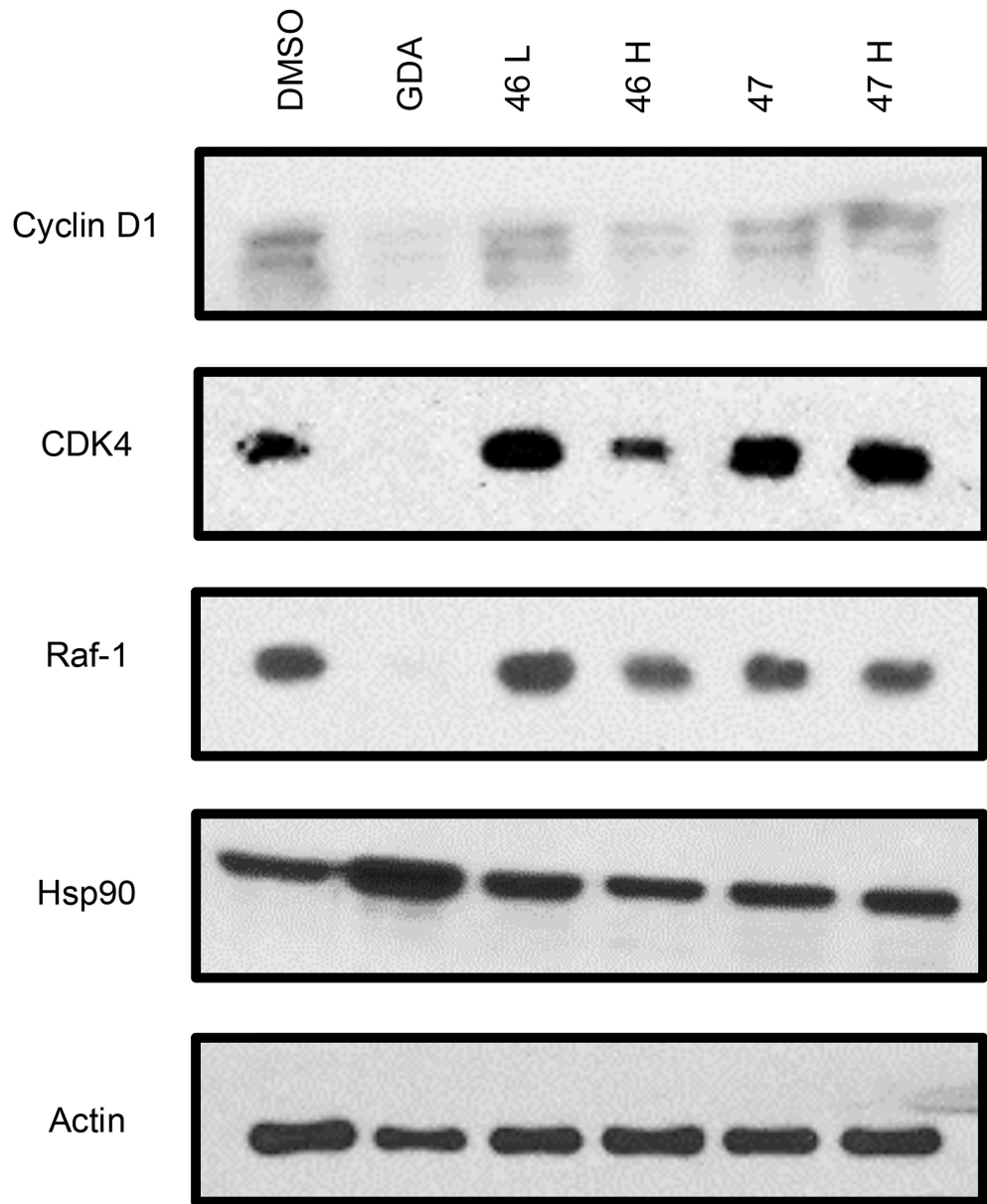
B.

Figure 3. Western blot analysis of Hsp90 client protein degradation in MCF-7 cells. Geldanamycin (GDA 500 nM) represents a positive control, while DMSO, represents the negative control. A. Analysis of cells treated with **44**. B. Analysis of cells treated with **45**.

A.



B.

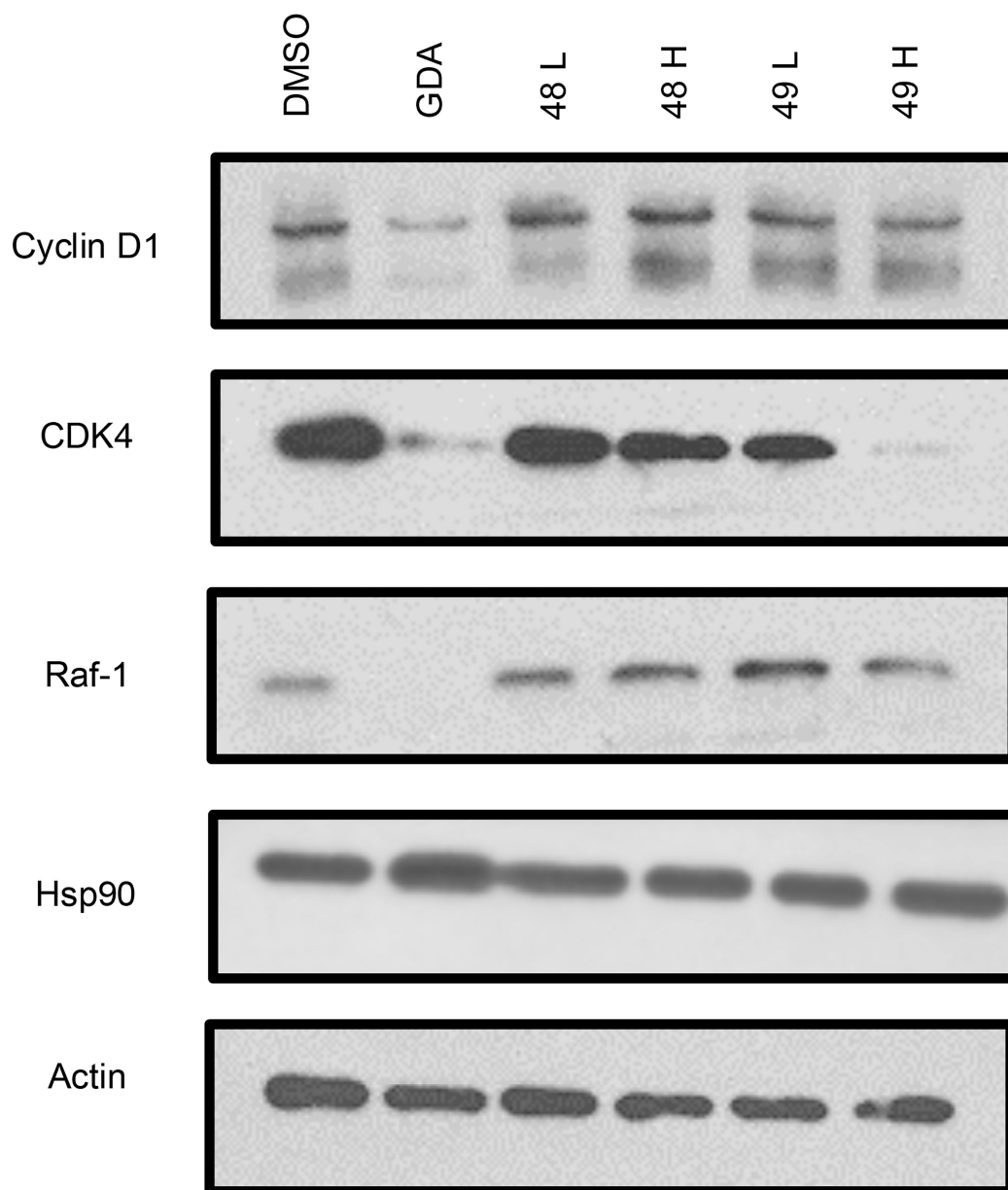
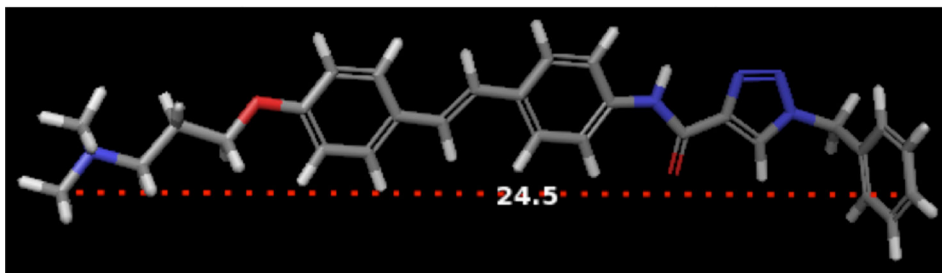
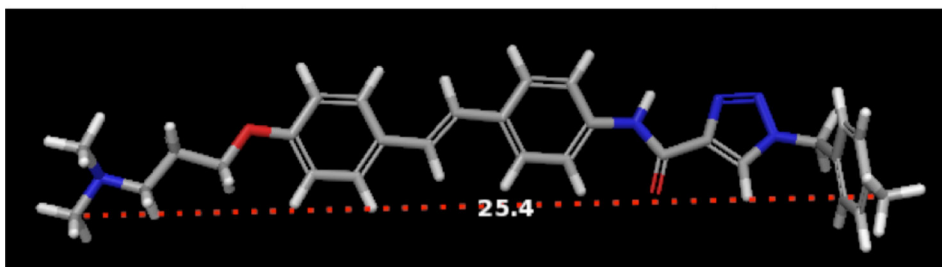


Figure 4. Western blot analysis of Hsp90 client protein degradation in MCF-7 cells treated with (A) **37** and **38** or (B) **39** and **40**. Geldanamycin (GDA 500 nm) represents a positive control, while DMSO, represents the negative control. L represents a concentration 1/2XIC50 value while H represents a concentration of 5XIC50 value.

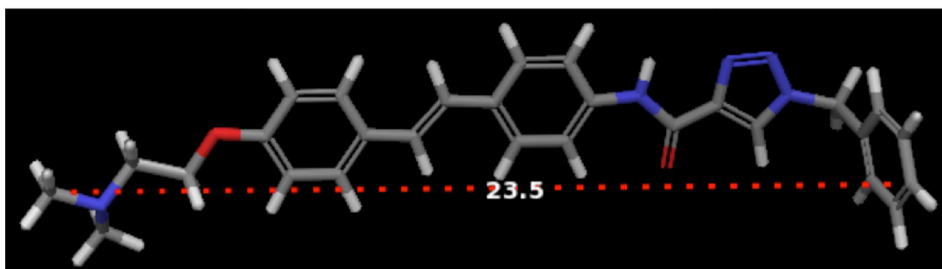
46



47



48



49

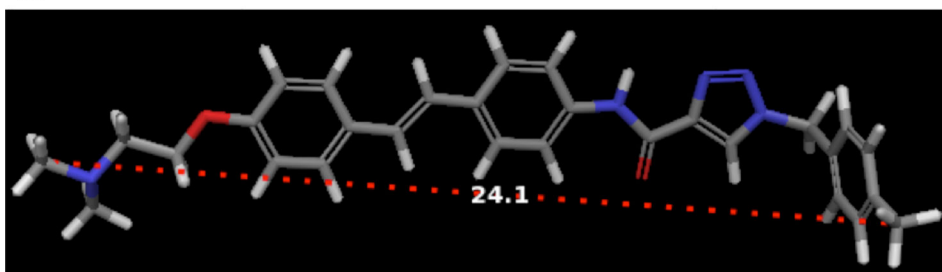
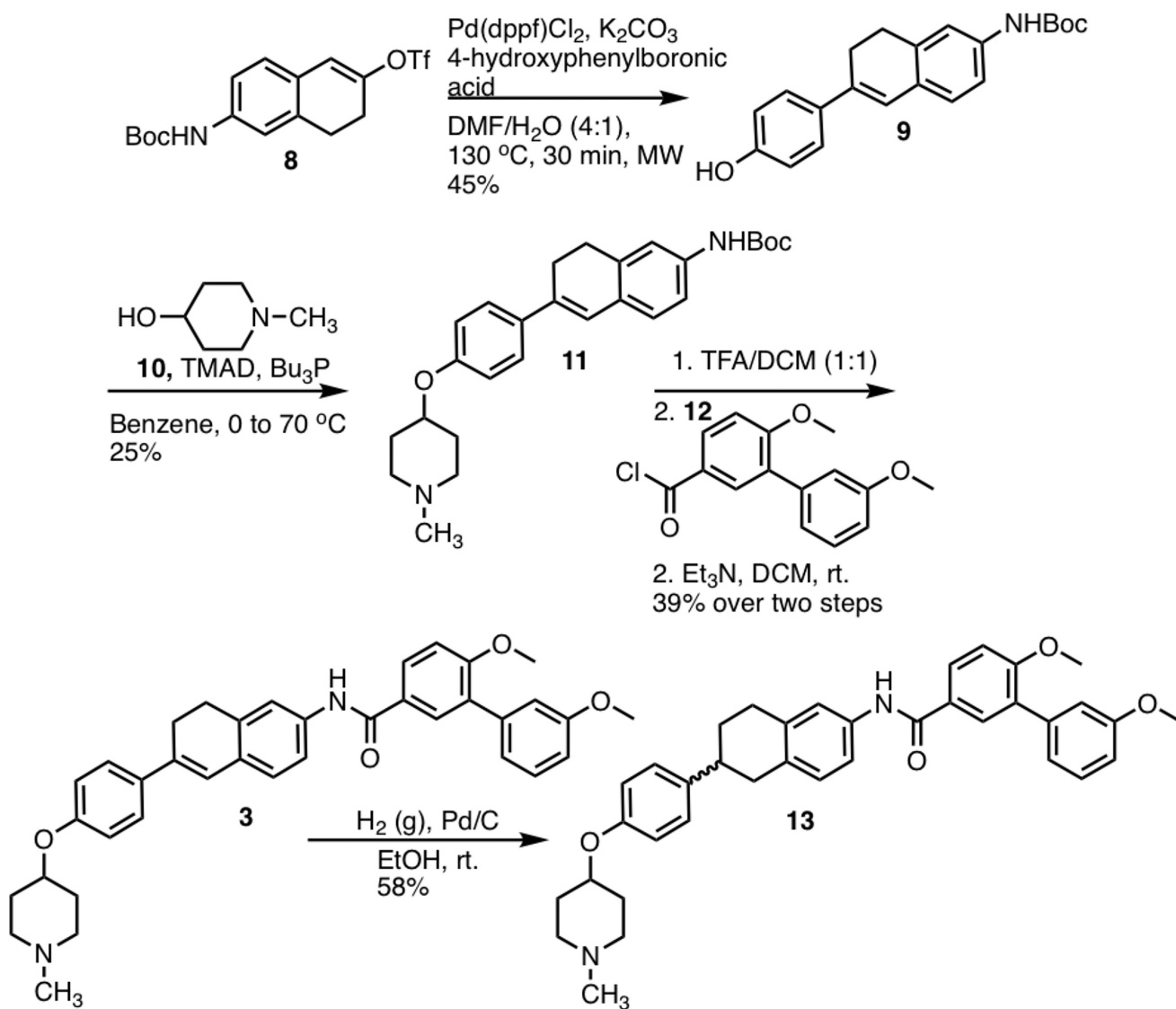
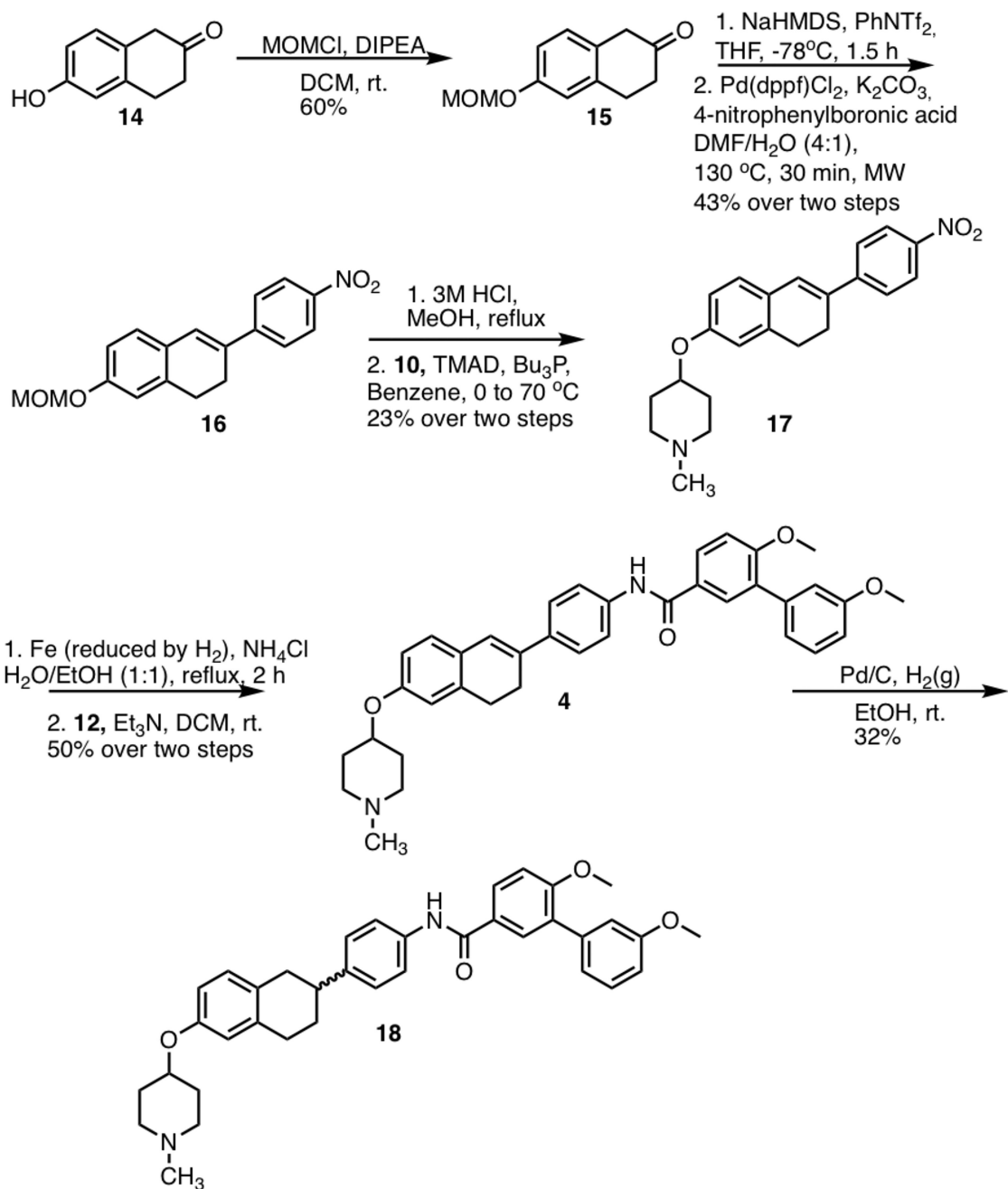


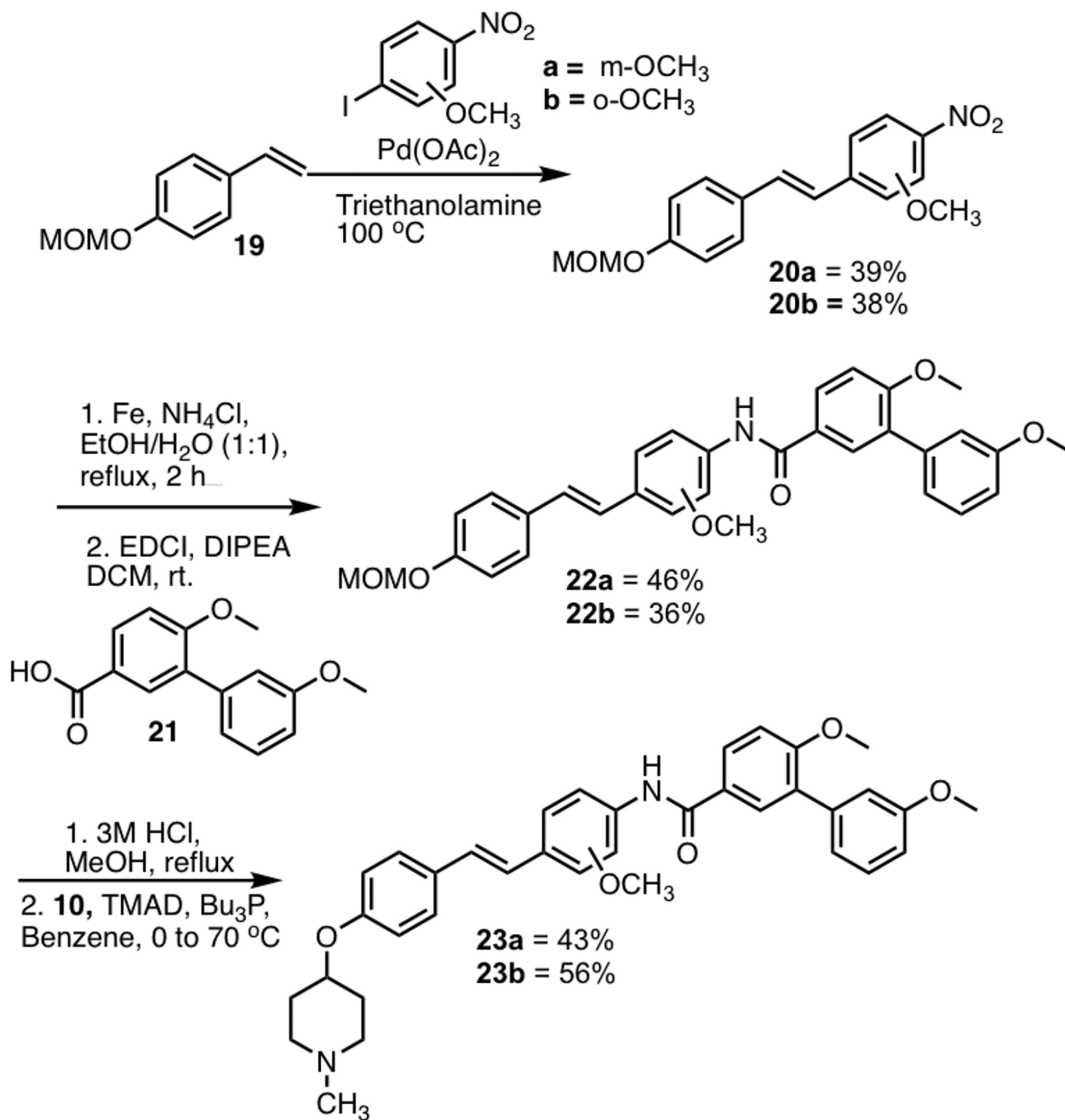
Figure 5. 3D structures of **46–49** with the length (Å) of each compound. A simple MM2 minimization was done in Chem3D^[36] for all of the compounds. The distance of the minimized structures were measured in Maestro.^[37]



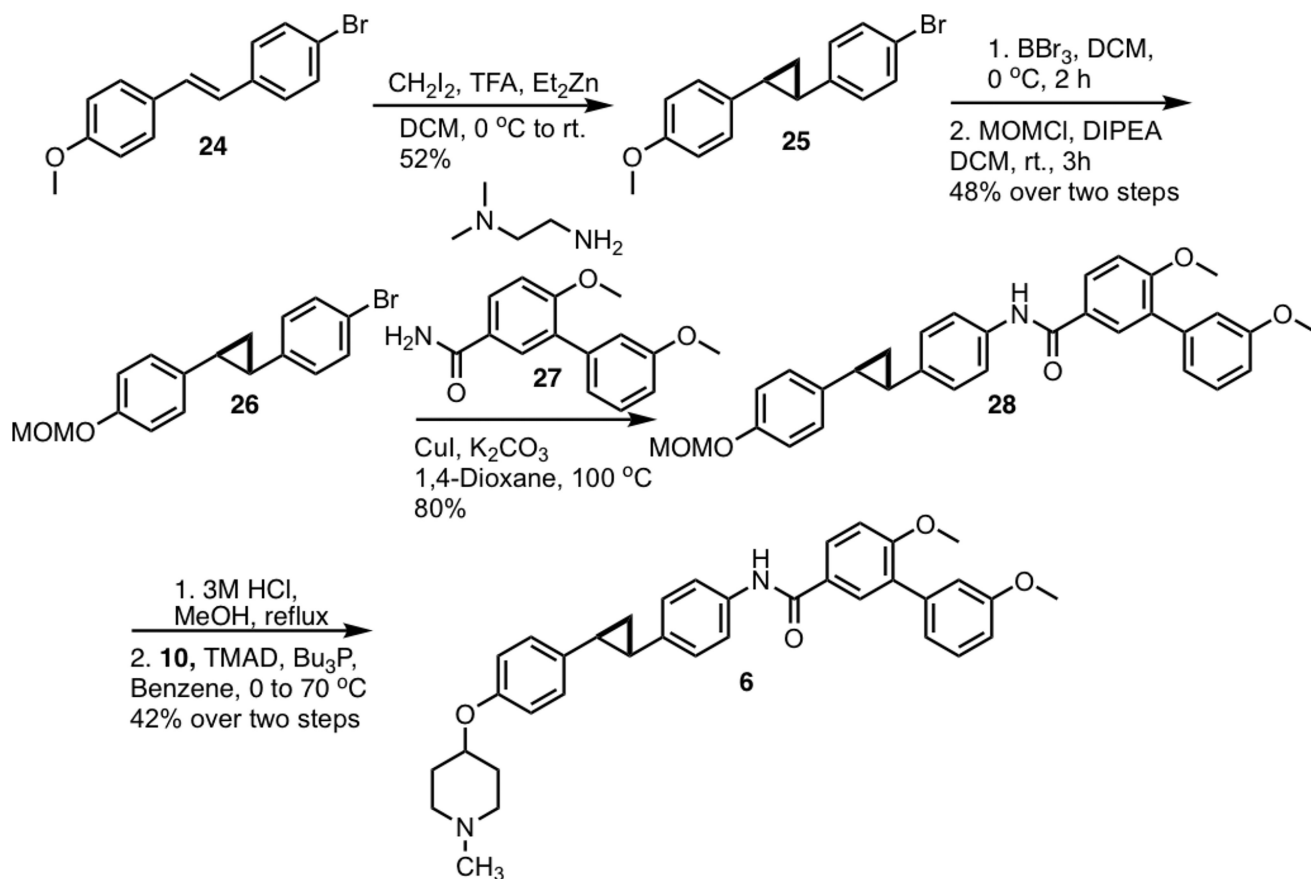
Scheme 1.
Synthesis of **3**



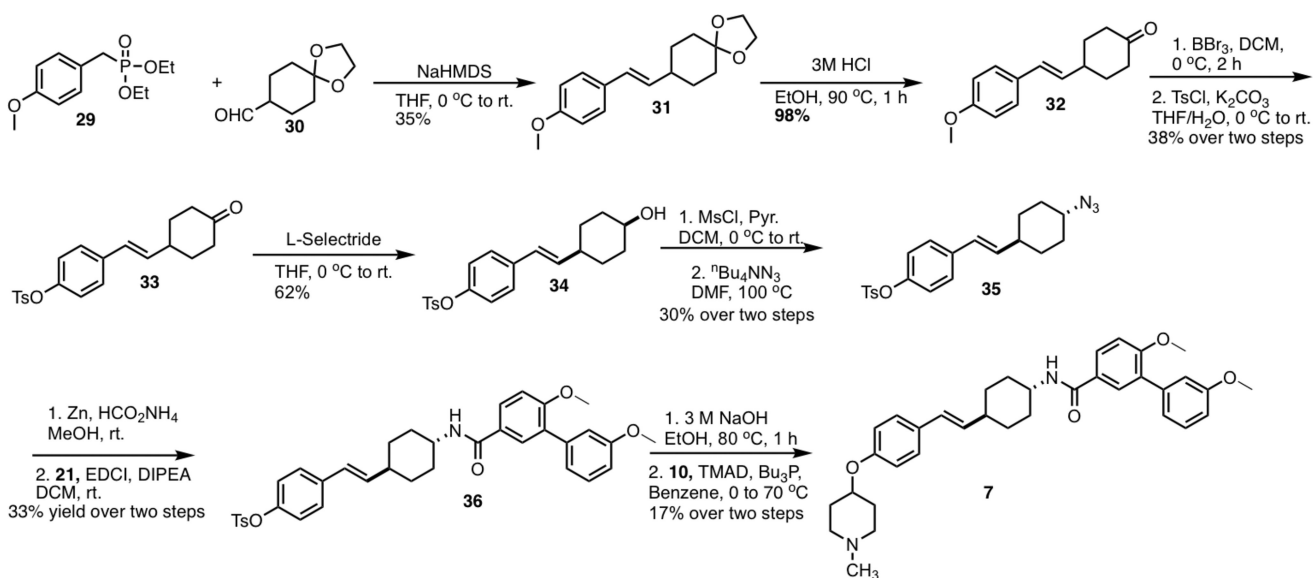
Scheme 2.
Synthesis of **4**



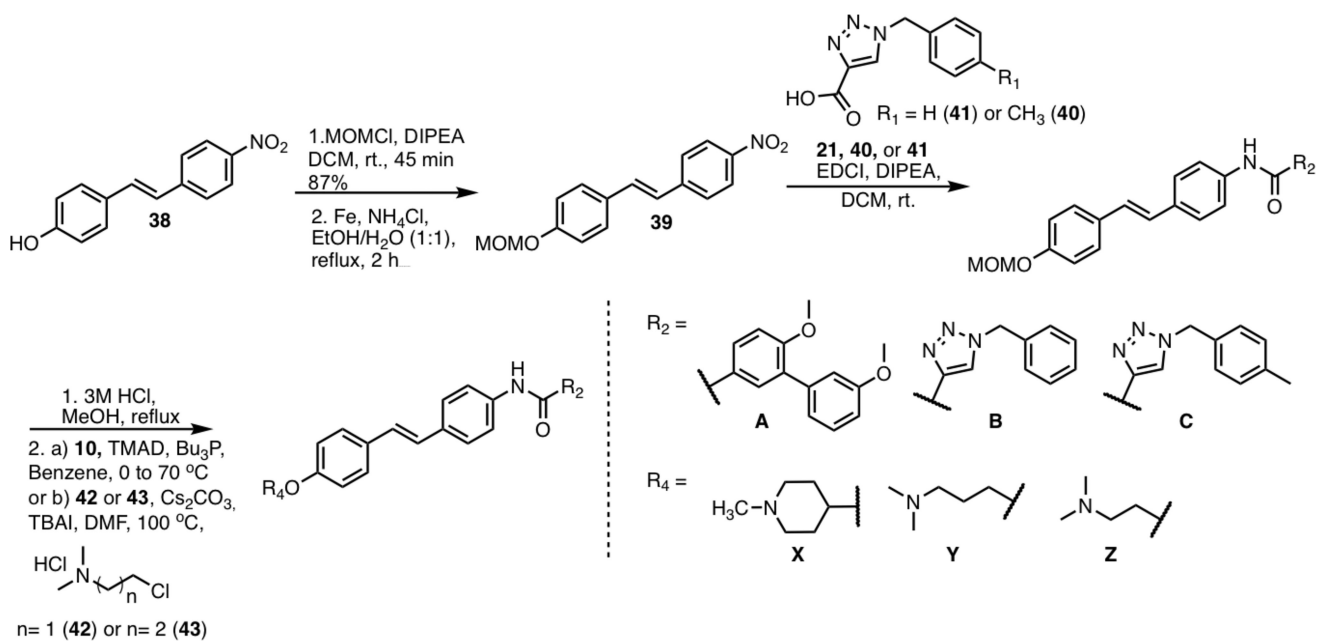
Scheme 3.
 Synthesis of **23a/b**



Scheme 4.
Synthesis of cyclopropane analog



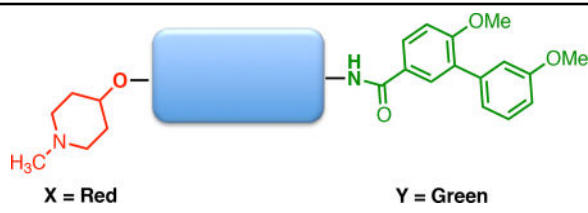
Scheme 5.
Synthesis of saturated analog of **2**

**Scheme 6.**

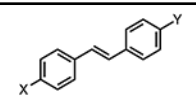
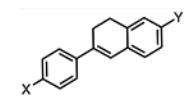
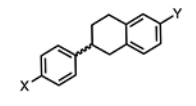
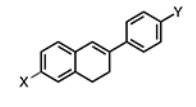
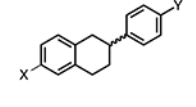
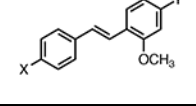
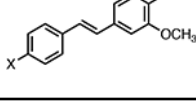
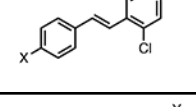
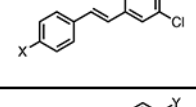
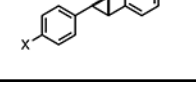
General Scheme for the preparation of second-generation stilbene analogs

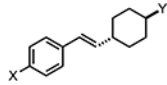
Table 1

Evaluation of anti-proliferative activity



X = Red Y = Green

Compound	Structure	MCF-7[a]	SKBr3[a]	HCT-116[a]
2		1.3±0.59	0.68±0.10	3.68±0.41
3		>50	>50	>50
13		>50	>50	>50
4		2.61±0.98	3.54±0.43	3.57±0.19
18		7.36±0.82	10.59±1.61	6.43±0.18
23a		3.59±0.068	3.64±0.20	4.50±0.99
23b		>50	>50	>50
37a		>50	>50	>50
37b		>50	27.46±0.057	>50
6		2.64±1.04	1.31±0.251	2.90±0.69

Compound	Structure	MCF-7 ^[a]	SKBr3 ^[a]	HCT-116 ^[a]
7		0.814±0.126	0.894±0.004	0.801±0.091

^[a] = Values are in μM , which represent mean standard deviation for at least two separate experiments performed in triplicate.

Table 2

Evaluation of biological activities of second-generation stilbene analogs

Compound	R ₄	R ₂	MCF-7[a]	SKBr-3[a]	HCT-116[a]
2	X	A	1.3±0.59	0.68±0.10	3.68±0.41
44	X	B	0.326±0.081	0.231±0.035	0.301±0.043
45	X	C	0.092±0.005	0.099±0.020	0.186±0.035
46	Y	B	0.325±0.034	0.382±0.101	0.350±0.064
47	Y	C	0.494±0.053	0.184±0.071	0.740±0.164
48	Z	B	0.234±0.052	0.183±0.003	0.350±0.064
49	Z	C	0.150±0.008	0.141±0.028	0.179±0.050
50	Y	A	5.86±1.23	9.68±0.209	5.51±0.225

[a] = Values are in μM , which represent mean standard deviation for at least two separate experiments performed in triplicate.